Korean J. Chem. Eng., **31**(11), 2094-2100 (2014)
DOI: 10.1007/s11814-014-0113-4

pISSN: 0256-1115
eISSN: 1975-7220

Entrainment of Geldart C particles in fluidized beds with binary particles

Joon Hwan Kim*, Jong Wook Bae*, JaeWook Nam*, Sang Done Kim, Jeong-Hoo Choi***, and Dong Hyun Lee*,†**

*School of Chemical Engineering, Sungkyunkwan University, 2066 Seobu-ro, Jangan, Suwon 440-746, Korea
**Department of Chemical and Biomolecular Engineering and Energy & Environment Research Center, Korea Advanced Institute of Science and Technology, Daejeon 305-701, Korea
***Department of Chemical Engineering, Konkuk University, Seoul 143-701, Korea
(*Received 12 January 2014 • accepted 16 April 2014*)

Abstract−The effects were determined of the mass ratio of Geldart C particles on the total amount of particles (M_{fine}/M_{total}=0-50 wt%), superficial gas velocity (U_g=0.5-1.0 m/s) and coarse particle size distribution (mono, binary, flat, and Gaussian type) on entrainment of Geldart C particles in a bubbling fluidized bed with binary particles (coarse particles: d_p=0.512 mm, ρ_s=2,339 kg/m^3 and Geldart C particles: d_p=13 μm, ρ_s=4,455 kg/m^3). The initial entrainment rate increases with increasing U_g. At U_g of 0.5 and 0.7 m/s, the initial entrainment rate slightly increases initially and then remains almost constant with increasing mass ratio (M_{fine}/M_{total}). At higher gas U_g of 0.85 and 1.0 m/s, the initial entrainment rate increases with increasing the mass ratio (M_{fine}/M_{total}) up to 30 wt%, after which the increasing slope of the initial entrainment rate decreases with increasing the mass ratio (M_{fine}/M_{total}). Also, the decrease in the coefficient of entrainment rate is equal to the increase in (M_{fine}/M_{total}) at the corresponding U_g. The average particle size of the entrained particles is about 12-16 μm at U_g of 0.5-1.0 m/s.

Keywords: Coarse Particle, Geldart C Particle, Fluidized Bed, Entrainment Rate Constant, Entrainment Rate

INTRODUCTION

Fluidized-bed technology [1] has been utilized for a number of chemical/physical processes in a relatively large scale by using relatively smaller solid particles. In a fluidized bed, particles are entrained outwardly along with gas flow once U_g exceeds their terminal velocity [2]. This particle entrainment is detrimental to the environment and the production process; therefore, it is an important parameter to consider in the process. In general, entrainment characteristics depend on the experimental conditions, such as the bed diameter, height, average particle size, particle size distribution, and gas flow rate [3]. Baron et al. [4] reported that fine particles not easily entrained due to the agglomeration phenomenon, particularly for fine particles that are mixed with silica sand and FCC. Baeyens et al. [5] also conducted an entrainment experiment with varying mass ratios of Geldart C to Geldart A particles and found that the coefficient of entrainment rate increased with decreasing size of the fine particles. Leva [6] reported that mass fraction of 5-20% is the range wherein the effect of the fine particles on the coefficient of entrainment rate is minimized. Wen and Hashinger [7] determined that the effect of fine particles on the coefficient of entrainment rate is minimal for weight fractions less than 25%. Ma et al. [8] reported that the effect of Geldart C particles on the coefficient of entrainment rate is minimal in a binary mixture system if it is less than 15%. Osberg and Charlesworth [9] stated that if the weight fraction of fine particles is in the range of 1-5%, the coefficient of entrainment rate is inversely proportional to the ratio of fine particles. However, Geldart et al. [10], Bashovchin et al. [11] and Smolders and Baeyens [12] claimed that the coefficient of entrainment rate increases as the mass fraction of fine particles increases. A number of experiments insisted that fine particles have an influence on the entrainment of the particles. However, the results varied significantly depending on the experimental conditions without any consistency in the results. In particular, there has not been any research on the entrainment characteristics by Geldart C particles depending on the distribution of the Geldart D and/or B particles. However, there have been few studies conducted on the entrainment of Geldart C particles with a broad range of gas velocities from 0.5 to 1.0 m/s. The previous studies are summarized in Table 1.

The objective of this study was to determine the initial entrainment rate and the coefficient of entrainment rate as a function of U_g and mass ratio (M_{fine}/M_{total}) in the bed, and also to determine the effect of coarse particle size distribution on the initial entrainment rate of Geldart C particles in a batch-type fluidized bed.

EXPERIMENTAL

1. Experimental Setup

Fig. 1 shows a schematic diagram of the experimental equipment for the entrainment experiment. Dry air passed through a dehumidifier was supplied to a fluidized bed (0.1 m-diameter×3.7 m-high). The entrained particles were collected by a cyclone. The particles not captured by the cyclone were collected in a bag filter. The weight of the entrained particles was measured with an electronic balance. An A/D converter (COMI-ZOA, SD202) was connected to a PC to read the weight of the entrained particles which were collected by the cyclone and converted the current to a voltage at 1 Hz for the elapsed time.

2. Samples

The experiment was conducted by using both coarse particles

†To whom correspondence should be addressed.
E-mail: dhlee@skku.edu

Table 1. Experimental conditions for entrainment of fine particles

Investigator	System	D_t [m]	Particles	Size of fine particle [m]	Size of coarse particle [m]	Initial wt. fraction of fine particle [wt%]	Gas velocity [m/s]	Remark
Wen and Hashinger [7]	Binary-multi system Batch	0.102	Glass bead Coal	7-10	28	6-100	0.50-0.96	Can be neglected (C_0<25%) $k \propto 1/C_0$ (C_0>25%)
Geldart et al. [10]	Multi-system Batch	0.076	Sand Alumina	62	219	5-75	1.48	$k^*_\infty \propto C_0$
Bachovchin et al. [11]	Binary, Multi-system continuous	0.15	Sand	22-210	600-109	10-20	0.61-1.25	$E \propto C_0$
Ma et al. [8]	Binary CFB	0.071	Limestone Silica sand	35-76 (Geldart A) 18 (Geldart C)	331	2-15 1-9	0.3-0.9	Can be neglected (C_0<15%) $k^*_\infty \propto 1/C_0$ (C_0<9%)
Smolders and Baeyens [12]	Multi-system Batch	0.082	Limestone Sand, Glass	16-74			0.1-0.8	$k^*_\infty \propto C_0$
Chyang et al. [16]	Binary, Multi-system Batch	0.19	Glass beads	49-194	545	2-32	1.18-1.75	$k^*_\infty \propto 1/C_0$ (C_0>16%) $k^*_\infty \propto C_0$ (C_0<16%)
Rodriguez et al. [18]	Binary-multi system Batch	0.046	Silica sand Iron oxide	0-74	149-210	9.1-13	0.15-0.38	
Li and Kato [14]	Binary CFB Steady-state	0.103	FCC Alumina PVC SiC Silica sand	12-91	69-650	10-20	0.3-0.7	Increase at bed diameter<60 μm Constant at bed diameter>200 μm
Li et al. [15]	Binary CFB Steady-state	0.103	Al(OH)3 Alumina TiO2 FCC Limestone SiC Silica sand	0.5-32	44-97	0-30	0.5	$k^*_\infty \propto 1/C_0$ (0-6 μm)

(Geldart B) and Geldart C particles with different particle sizes and densities. For the coarse particles, glass beads were used (d_p=0.512 mm, ρ_s=2,339 kg/m^3). While keeping a Sauter mean diameter constant of 0.512 mm, the experiment was conducted by varying the particle size distribution with mono, binary, flat and Gaussian types, as shown in Fig. 2 and Table 2. The resolution was kept constant at 0.34 in order to design the particle size distribution of the coarse particles. The coarse particles have a smooth globular surface, as shown in Fig. 3(a). Geldart C particles (d_p=13 μm, ρ_s=4,455 kg/m^3) were used after passing them through a sieve with a size of less than 37 μm, as shown in Fig. 4. Due to their small sizes, particle sizes were analyzed by a wet particle size analyzer. The basic properties of the samples are shown in Table 3. The Geldart Group C particles are smaller with a relatively higher density than that of the coarse particles, so that the cohesiveness of the particles is strong. Fig. 3(b) is an SEM image showing the shape of the Geldart C particles. The particles are not round but flat-plane shape. The samples were completely dried in an oven at 400 K for 24 h before use.

3. Experimental Procedure

To determine the effect of size distribution of coarse particles on entrainment, the experiment was conducted by changing the distribution of particle size to mono, binary, flat, and Gaussian types, while consistently maintaining a Sauter mean diameter of 0.512 mm. To check the entrainment characteristics by varying the mass ratio (M_{fine}/M_{total}), the mass ratio increased from 0 to 50% at U_g in the range of 0.5-1.0 m/s to calculate the initial entrainment rate, the coefficient of entrainment rate, etc. The initial amount of particles loaded into the beds was kept at 4 kg.

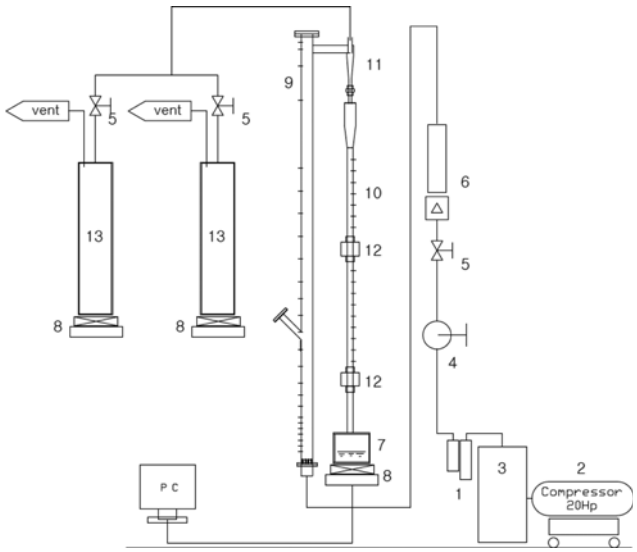

Fig. 1. Experimental setup.

1. Air filter
2. Compressor
3. Air dryer
4. Regulator
5. Valve
6. Rota meter
7. Sampling vessel
8. Electric balance
9. Main column
10. Pressure tap
11. Cyclone
12. Block valve
13. Bag filter

4. Data Analysis

As shown in Table 1, a number of studies have been carried out on the entrainment of Geldart C particles. Based on these studies, the coefficients of entrainment rate and entrainment as a function of time were calculated by using the equation of Wen and Hashinger [7] and comparing the calculated values with the experimental ones.

The Geldart C particles are entrained with time so that concentration of the Geldart C particles varies with elapsed time.

$$\frac{dC}{dt} = -kC \tag{1}$$

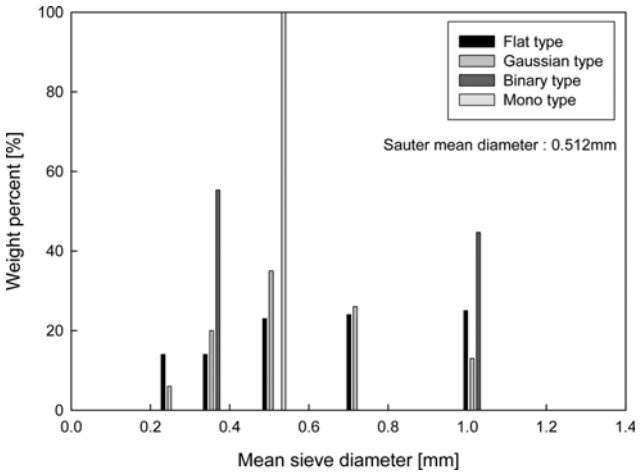

Fig. 2. Coarse particle size distribution.

$$C = \frac{w_0 - w}{W_t - w} \tag{2}$$

$$k = \frac{KA}{W_t - w} \tag{3}$$

where W_t is the amount of particles loaded into the bed and w_0 is initial mass of fine particles. w is a time-based variable, which is the amount of entrained particles. Substituting Eq. (2) into Eq. (1) and replacing the entrainment rate with the coefficient of entrainment rate leads to Eq. (4).

$$\frac{dC}{dt} = \frac{w_0 - W_t}{(W_t - w)^2}\frac{dW}{dt} = -k\frac{w_0 - w}{W_t - w} \tag{4}$$

Integrating Eq. (4) and using Eq. (3), Eqs. (5) and (6) are derived.

$$\ln(w_0 - w) = -KA\frac{1}{(W_t - w_0)}t + \ln w_0 \tag{5}$$

$$w = w_0\left(1 - e^{\frac{-KAt}{W_t - w_0}}\right) \tag{6}$$

Table 2. Standard deviation and variance of typical types of the bed materials

PSD*	Sieves [mm]	Average diameter [mm]	Cumulative weight, Ø [%]	ΔØ	σ [mm]	σ^2 [mm^2]
Gaussian	0.212-0.300	0.256	6	6	0.230	0.053
	0.300-0.425	0.3625	26	20		
	0.425-0.600	0.5125	61	35		
	0.600-0.850	0.725	87	26		
	0.850-1.190	1.050	100	13		
Flat	0.212-0.300	0.256	14	14	0.294	0.086
	0.300-0.425	0.3625	25	14		
	0.425-0.600	0.5125	51	23		
	0.600-0.850	0.725	75	24		
	0.850-1.190	1.050	100	25		
Binary	0.300-0.425	0.3625	55.3	55.3	0.356	0.127
	0.850-1.190	1.050	100	44.7		
Mono	0.425-0.600	0.5125	100	100	0	0

*PSD: particle size distribution

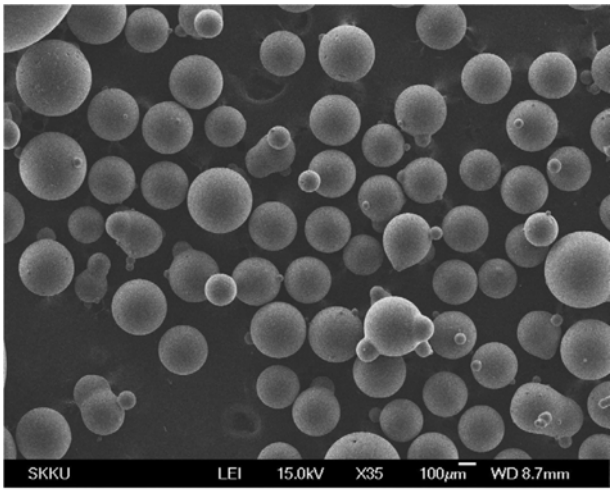

(a)

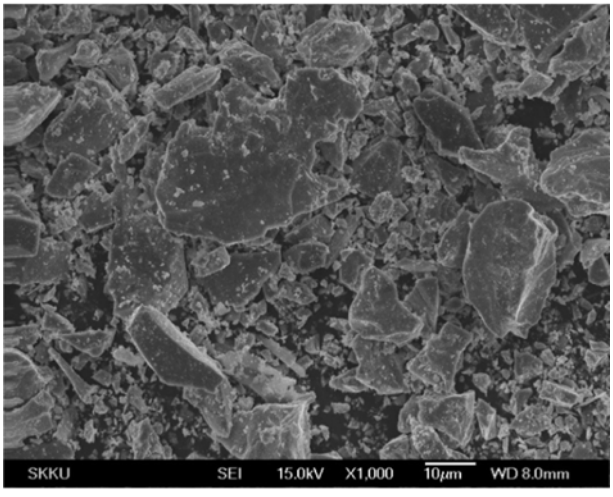

(b)

Fig. 3. SEM images of used particles: (a) Coarse particles and (b) Geldart C particles.

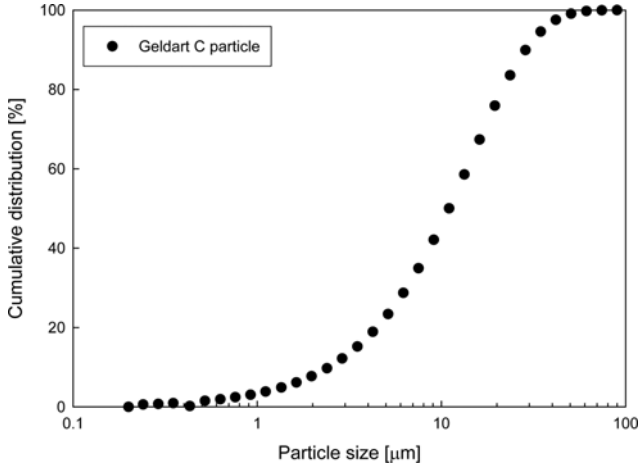

Fig. 4. Cumulative particle size distribution of Geldart C particles.

It is possible to compare the experimental value with the entrainment calculated by using Eq. (6).

Table 3. Physical properties of bed materials

Material	Mean diameter [mm]	True density [kg/m^3]	Bulk density [kg/m^3]	Voidage [-]
Coarse particles	0.512	2,339	1,482	0.366
Geldart C particles	0.013	4,455	2,374	0.467

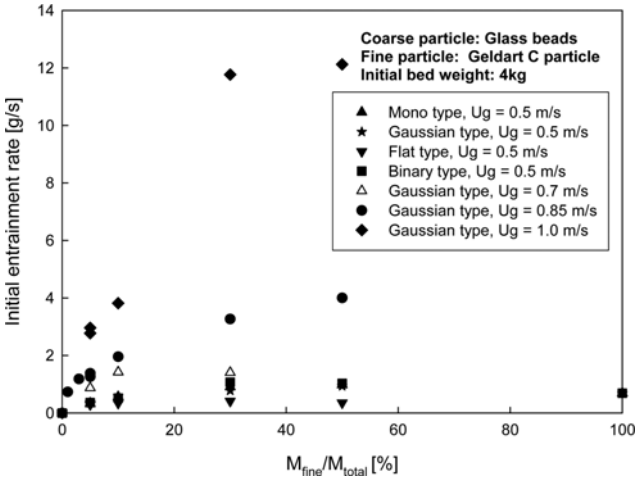

Fig. 5. Variation of initial entrainment rate with the mass ratio of Geldart C particles to total particles.

Also, it is a batch mode experiment, so the initial entrainment rate, k_0, can be calculated from the initial slope of the entrainment rate.

The percentage of entrainment, E, is defined and calculated as:

$$E = \frac{w_\infty}{w_0} \tag{7}$$

The particle size of the entrained particles was measured by using a wet particle-size analyzer.

RESULTS AND DISCUSSION

The initial entrainment rate as a function of the mass ratio (M_{fine}/M_{total}) is shown in Fig. 5. It was anticipated that the initial entrainment rate increases with increasing the amount of Geldart C particles in the bed. However, as can be seen in Fig. 5, at U_g of 0.5 m/s, the initial entrainment rate slightly increased initially and then remained almost constant with increasing mass ratio (M_{fine}/M_{total}). At higher gas U_g of 0.85 and 1.0 m/s, the initial entrainment rate increased with increasing the mass ratio (M_{fine}/M_{total}) up to 30 wt%, after which the increasing slope of the initial entrainment rate decreased with increasing the mass ratio (M_{fine}/M_{total}). The Geldart C particles are likely to agglomerate, due to their small size and large surface area. Therefore, if the amount of Geldart C particles increases over a certain level at U_g of 0.5 and 0.7 m/s, the entrainment rate does not increase in proportion to the mass ratio (M_{fine}/M_{total}). When the mass ratio (M_{fine}/M_{total}) was less than 30% at U_g of 0.85 or 1.0 m/s, the entrainment rate increased initially and then remained almost constant. At U_g of 0.85 m/s, it is found that the clusters of Geldart C particles (formed by adhesion) were broken, because the hydrodynamic force

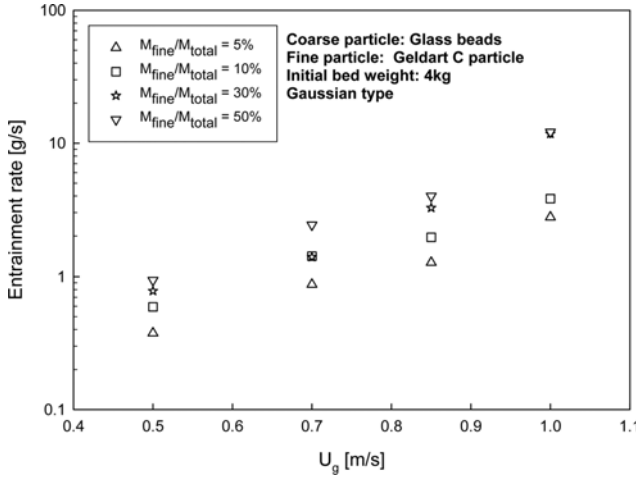

Fig. 6. Variation of the initial entrainment rate with the superficial gas velocity in the case of the coarse particles of the Gaussian type.

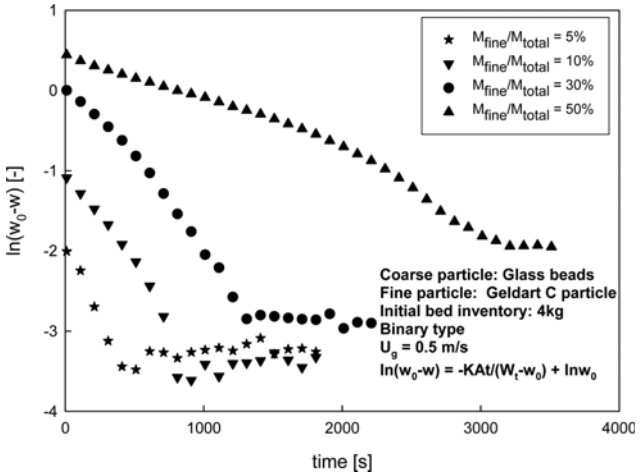

Fig. 8. Variation of $\ln[(w_0-w)]$ with the elapsed time in the batch type fluidized beds with the coarse particles of the binary type.

is an important factor affecting the entrainment. Kage et al. [13] reported that the initial entrainment rate reaches a constant value once the mass ratio (M_{fine}/M_{total}) increases over a certain level, because those particles that already have been floating were disturbed by the particles below. Therefore, there is a clear difference between the initial entrainment rate at U_g of 0.5 and 0.7 m/s and the initial entrainment rate of the Geldart C particles at higher U_g of 0.85 and 1.0 m/s.

Variation of the initial entrainment rate with U_g in the bed of coarse particles with Gaussian type distribution is shown in Fig. 6. Previous studies reported that the entrainment rate increased with increasing U_g [7,14]. Kato et al. [14] reported that the slip velocity was the most important factor affecting the entrainment characteristics of particles, which is equal to the difference between U_g and particle terminal velocity.

The effect of the mass ratio (M_{fine}/M_{total}) on the percentage of entrainment is shown in Fig. 7. At U_g of 0.5 and 0.7 m/s, the percentage entrainment gradually decreases with increasing mass ratio (M_{fine}/M_{total}) due to the cohesive force between the coarse particles and Geldart C particles. However, at superficial gas velocities over 0.85 m/s, the percentage entrainment increased initially and then remained almost constant with increasing the mass ratio of (M_{fine}/M_{total}), because U_g is the factor having the most influence on the entrainment and particle mixing.

Variation of $\ln[(w_0-w)]$ with the elapsed time in the batch mode fluidized beds of binary coarse particles by using Eq. (5) is shown in Fig. 8. Because it is a batch-type fluidized bed, it is possible to calculate the slope, which can be used later in calculating the coefficient of entrainment rate, using the initial slope. As can be seen in Fig. 8, the value of $\ln[(w_0-w)]$ decreased with increasing elapsed time and then remained constant with a further increase in elapsed time.

The effect of the mass ratio (M_{fine}/M_{total}) on the coefficient of entrainment rate is shown in Fig. 9. As the mass ratio (M_{fine}/M_{total}) was increased, the coefficient of entrainment rate decreased. Li et al. [15] reported that the coefficient of entrainment rate decreased with increasing mass ratio (M_{fine}/M_{total}), because the Geldart C particles are likely to agglomerate with each other and become attached to

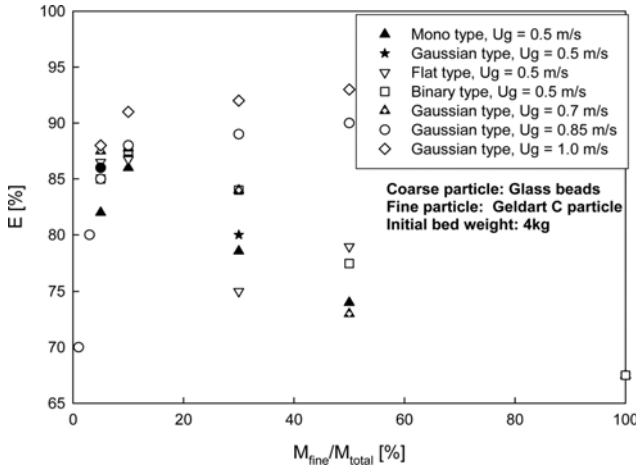

Fig. 7. Variation of the percentage entrainment with the mass ratio of Geldart C particles to total particles.

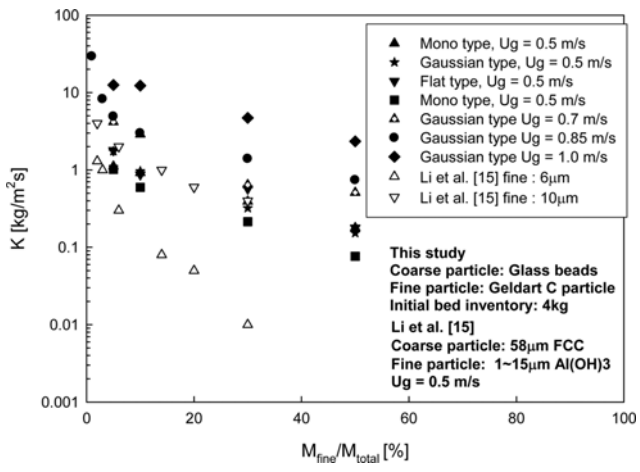

Fig. 9. Effect of the mass ratio of Geldart C particles to total particles on the coefficient of entrainment rate.

the coarse particles. Chyang et al. [16] determined the coefficient of entrainment rate based on the mass ratio (M_{fine}/M_{total}). They reported that the coefficient of entrainment rate would decrease at a mass ratio (M_{fine}/M_{total}) up to 16% and increase thereafter. Sun and Grace [17] stated that the momentum required to entrained particles on the bed surface decreased with increasing mass ratio (M_{fine}/M_{total}), due to the decrease in both the average particle size in the beds and the bubble size at the corresponding U_g. In general, according to the two-phase theory, bubble frequency decreases once the bubble size increases at a corresponding U_g. As the mass ratio of Geldart A fine particles increases at the same U_g, bubble frequency increases. As can be expected, bubble frequency decreases with increasing bubble size; the coefficient of entrainment rate increases with increasing the mass ratio (M_{fine}/M_{total}) since it is affected more by the former than by the latter at mass ratios (M_{fine}/M_{total}) over 16%. For Geldart C particles, the average particle size in the beds decreases with increasing mass ratio (M_{fine}/M_{total}). Therefore, the flow characteristics in the beds become smooth and the momentum of particles can decrease. In addition, as the mass ratio (M_{fine}/M_{total}) increases, there will be more agglomeration occurs that may decrease the coefficient of entrainment rate.

The effect of U_g on the coefficient of entrainment rate (K) is shown in Fig. 10 where the coefficient of entrainment rate increases with increasing gas velocity. Chyang et al. [16] reported that the coefficient of entrainment rate is a strong function of Froude Number, as shown below:

$$\frac{K}{\rho_g U_t} = aFr^{1.32} \tag{8}$$

$$Fr = \frac{(U_g - U_t)^2}{g d_{p,f}}, \quad 0 \le d_{p,f} \le 37\ \mu m, \quad 0.5 \le U_g \le 1.0\ m/s \tag{9}$$

The coefficient of entrainment rate obtained by changing the particle size distribution of coarse particles at U_g of 0.5 m/s is shown in Fig. 11. Sun and Grace [17] reported that the bubble size varied if the particle size distribution changed, although they kept the average particle size constant to make it easier to transfer from the bubbling fluidization regime to the turbulent fluidization regime in a wide size distribution than in a narrow size distribution. Therefore, as the particle distribution of the coarse particles varied, the flow pattern changed at the corresponding U_g. However, this change did not have much influence on the particle entrainment. The reason for this is that the total surface area of coarse particles is the same if they have the same average particle size, so that there is no difference in the amount of Geldart C particles that adhere to the coarse particles. However, the flat type particles (σ^2=0.086) have a smaller coefficient of entrainment rate than the other types, such as the Gaussian (σ^2=0.053) and binary (σ^2=0.127) types, because the smallest particles among the coarse particles is more than other types.

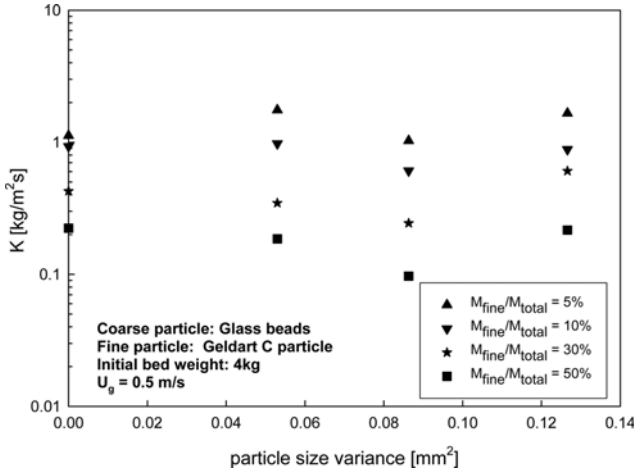

Fig. 11. Coefficient of entrainment rate obtained by changing the particle size distribution of the coarse particles at a gas velocity of 0.5 m/s.

The average particle size of the entrained particles and that of the particles attached to the surface of the glass beads is shown in Fig. 12. The average particle size indicates that the entrained particles have a diameter of about 12-16 μm. The amount of agglomerated particles varies depending on the mass ratio and gas velocity, but it was found that the average particle diameter of the entrained particles was similar that of the original Geldart C particles before the experiment. A sample of 100 g of glass beads was found to contain

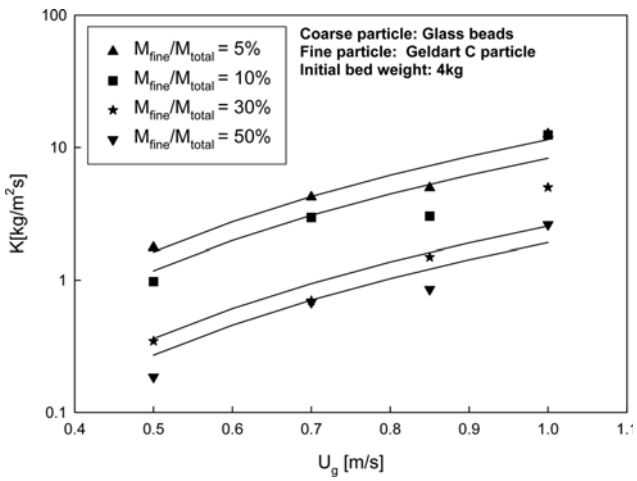

Fig. 10. Effect of superficial gas velocity on the coefficient of entrainment rate.

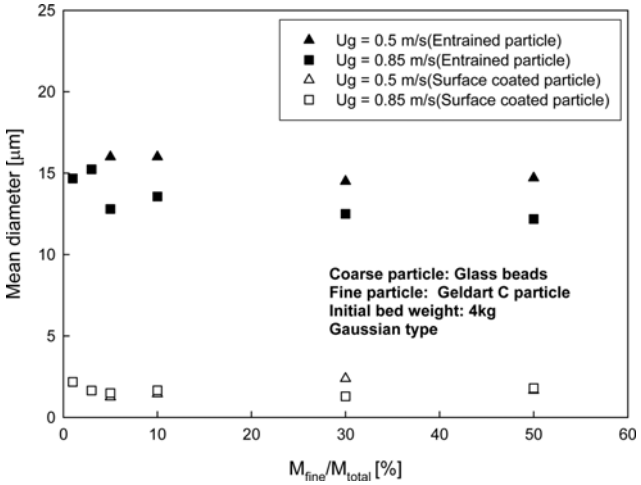

Fig. 12. Average particle size of entrained particles and that of the particles attached to the surface of the glass beads.

free-floating Geldart C particles in the bed. Therefore, it is necessary to separate the glass beads from the Geldart C particles with a 125 μm sieve for 5 minutes. Then the particles were agitated for 10 min with a magnetic bar to separate the Geldart C particles from the surface of the glass beads. Geldart C particles with an average particle size of 1.5-2.5 μm were attached to the surface. Also, the maximum size of the particles that were attached to the surface of the glass beads was found to be about 5-7 μm.

CONCLUSION

The entrainment characteristics (initial entrainment rate, percentage entrainment and coefficient of entrainment rate) of Geldart C particles were determined in a 0.1 m-ID×3.7 m-high fluidized bed of binary particles.

(1) At U_g of 0.5 and 0.7 m/s, the initial entrainment rate slightly increased initially and then remained almost constant with increasing mass ratio of Geldart C particles to the total mass of particles in the bed.

(2) At higher U_g of 0.85 and 1.0 m/s, the initial entrainment rate increased with increasing mass ratio (M_{fine}/M_{total}) up to 30 wt% and then the increasing slope of the initial entrainment rate decreased with increasing the mass ratio (M_{fine}/M_{total}).

(3) At U_g of 0.5 and 0.7 m/s, the percentage entrainment gradually decreased with increasing mass ratio of Geldart C particles to total particles. However, at superficial gas velocities over 0.85 m/s, the percentage entrainment was increased initially and then remained almost constant with increasing the mass ratio (M_{fine}/M_{total}).

(4) The flat type of particles (σ^2=0.294) have a smaller coefficient of the entrainment rate than the other types of particles such as the Gaussian (σ^2=0.230) and binary (σ^2=0.356) types.

(5) The average particle diameter of the entrained particles at U_g of 0.5-1.0 m/s is about 12-16 μm. The average size of the particles attached to the surface of the glass beads is about 1.5-2.5 μm. Also, the maximum size of the particles that are attached to the surface of the glass beads is about 5-7 μm.

NOMENCLATURE

a : constant of Eq. (8) [-]
A : effective cross-sectional area of bed [m^2]
C : fine particle concentration [%]
$d_{p,f}$: fine particle concentration [m]
d_p : particle mean diameter [m]
D_t : column diameter [m]
E : percentage entrainment [%]
Fr : froude number [-]
g : gravity acceleration [m/s^2]
k : entrainment rate [1/s]
k_0 : initial entrainment rate [1/s]
K : coefficient of entrainment rate [kg/m^2s]
M_{fine}/M_{total} : mass ratio of fine to coarse particle [%]
t : time [s]
U_g : superficial gas velocity [m/s]
U_t : terminal velocity of particles [m/s]
w : entrainment weight at a certain time [kg]
w_0 : initial fine particle weight [kg]
w_∞ : total entrained mass of fine particle [kg]
W_t : total bed weight [kg]
Ø : cumulative weight [%]
σ : standard deviation [mm]
σ^2 : variance [mm^2]
ρ_s : particle density [kg/m^3]

REFERENCES

1. S. W. Kim, W. Namkung and S. D. Kim, *Theories Appl. Chem., Eng.*, **2**, 2339 (1996).
2. D. Kunii and O. Levenspiel, *Fluidization engineering*, Butterworth-Heinemann, Boston (1991).
3. X. Ma and K. Kato, *Powder Technol.*, **95**, 93 (1998).
4. T. Baron, C. L., J Bariens, J. D. Hazlett, M. A. Bergougnou and P. Galtier, *Powder Technol.*, **70**, 631 (1992).
5. J. Baeyens, D. Geldart and S. Y. Wu, *Powder Technol.*, **71**, 71 (1992).
6. M. Leva, *Chem. Eng. Progress*, **47**, 39 (1951).
7. C. Y. Wen and R. F. Hashinger, *AIChE J.*, **6**, 220 (1960).
8. X. Ma, Y. Honda, N. Nakagawa and K. Kato, *J. Chem. Eng. Japan*, **29**, 330 (1996).
9. G. L. Osberg and K. H. Charlesworth, *Chem. Eng. Progress*, **47**, 566 (1951).
10. D. Geldart, J. Cullinan, S. Georghiades, D. Gilvray and K. J. Pope, *Trans. Inst. Chem. Eng.*, **57**, 269 (1979).
11. D. M. Bachovchin, J. M. Beer and A. F. Sarofim, *AIChE Symp. Ser.*, **205**, 76 (1981).
12. K. Smolders and J. Baeyens, *Powder Technol.*, **92**, 35 (1997).
13. H. Kage, M. Tsumori and Y. Matsuno, *J. Chem. Eng. Japan*, **24**, 33 (1991).
14. J. Li and K. Kato, *Powder Technol.*, **118**, 209 (2001).
15. J. Li, T. Nakazato and K. Kato, *Chem. Eng. Sci.*, **59**, 2777 (2004).
16. C. S. Chyang, H. P. Wan and Y. C. Liu, *J. Chem. Eng. Japan*, **31**, 950 (1998).
17. G. Sun and J. R. Grace, *AIChE J.*, **38**, 716 (1992).
18. J. M. Rodriguez, J. R. Sanchez, A. Alvaro, D. F. Florea and A. M. Estevez, *Powder Technol.*, **111**, 218 (2000).